Journal of Cell Science 111, 3645-3654 (1998)
Printed in Great Britain © The Company of Biologists Limited 1998
JCS0041

The presenilin protein family member SPE-4 localizes to an ER/Golgi derived organelle and is required for proper cytoplasmic partitioning during *Caenorhabditis elegans* spermatogenesis

P. Michele Arduengo[1,*], Ollie Kelly Appleberry[2,‡], Peale Chuang[2,§] and Steven W. L'Hernault[1,¶]

[1]Graduate Program in Biochemistry and [2]Department of Biology, Cell and Developmental Biology, Emory University, Atlanta, Georgia 30322, USA

*Present address: Department of Biology, Morningside College, Sioux City, Iowa 51106, USA

†Present address: Department of Physiology, Emory University School of Medicine, Atlanta, Ga 30322, USA

§Present address: University of Colorado Health Science Center, Denver, CO 80262, USA

¶Author for correspondence (e-mail: bioslh@biology.emory.edu)

Accepted 21 October; published on WWW 18 November 1998

SUMMARY

During *Caenorhabditis elegans* spermatogenesis, asymmetric partitioning of cellular components principally occurs via ER/Golgi-derived organelles, named fibrous body-membranous organelles. In *C. elegans spe-4* mutants, morphogenesis of fibrous body-membranous organelle complexes is defective and spermatogenesis arrests at an unusual cellular stage with four haploid nuclei within a common cytoplasm. The *spe-4* encoded integral membrane protein is a diverged member of the presenilin family implicated in early onset Alzheimer's disease. Specific antisera were used to show that SPE-4 resides within the fibrous body-membranous organelles membranes during wild-type spermatogenesis. Several *spe-4* recessive mutants were examined for SPE-4 immunoreactivity and a deletion mutant lacks detectable SPE-4 while either of two missense mutants synthesize and localize immunoreactive SPE-4 within their fibrous body-membranous organelles. One of these missense mutations is located within a motif that is common to all presenilins. *spe-4* mutants were also examined for other partitioning defects and tubulin was found to accumulate in unusual deposits close to the plasma membrane. These results suggest that wild-type SPE-4 is required for proper localization of macromolecules that are subject to asymmetric partitioning during spermatogenesis.

Key words: Membrane, Spermatogenesis, Presenilin, Tubulin, *Caenorhabditis elegans*

INTRODUCTION

The asymmetric partitioning of cellular components during cellular divisions is a central feature of differentiation, yet the mechanism establishing asymmetry is poorly understood. Asymmetric segregation of cellular components occurs during *Caenorhabditis elegans* spermatogenesis, and this system is amenable to genetic, cytological, and biophysical analyses (reviewed by L'Hernault, 1997). Many components necessary for spermatid differentiation are segregated within the Golgi/ER derived fibrous body-membranous organelle (FB-MO) complexes (see Fig. 1; Wolf et al., 1978; Ward et al., 1981; Roberts et al., 1986; Ward, 1986). Several of the over 60 different spermatogenesis-defective (*spe*) mutants identified in *C. elegans* affect the morphogenesis and/or proper partitioning of FB-MOs (reviewed by L'Hernault, 1997). Analyses of the proteins encoded by these genes should reveal how the asymmetric distribution of cellular components occurs and its relationship to sperm differentiation.

In wild-type cells, the fibrous bodies (FB) form in close association with the membranous organelles (MO) as the primary spermatocyte develops, and they remain stably associated with the MOs until the spermatid is formed (Fig. 1). The FB-MO complexes are later segregated specifically into developing spermatids. Fibers in the FB are major sperm protein (MSP), and these fibers depolymerize in spermatids to disperse MSP dimers (Klass and Hirsh, 1981) throughout the cytoplasm (Roberts et al., 1986). After FB disassembly, the vesicular MOs localize under the cell surface and subsequently fuse with the plasma membrane to form permanent fusion pores during spermiogenesis. This membrane fusion event leads to exocytosis of MO contents onto the spermatozoon cell surface (Fig. 1).

All *spe-4* mutants produce spermatocytes that contain ultrastructurally disrupted FB-MOs (L'Hernault and Arduengo, 1992). Unlike wild-type, the FB in *spe-4* mutants does not show a stable association with the double layered membrane of the MO. Instead, FBs show no obvious association with MO membranes during their assembly so if such an association occurs, it is transient in *spe-4* mutants. The highly distended and abnormally vacuolated MOs in *spe-4* spermatocytes are throughout the cytoplasm rather than under

the cell surface as in wild-type cells. These FB-MO defects are associated with defective cell division, and a spermatocyte containing four haploid nuclei within a common cytoplasm is the last observed stage; spermatids never form in null *spe-4* mutants (Fig. 1; L'Hernault and Arduengo, 1992).

The *spe-4* gene encodes a 465 residue protein that contains at least seven predicted transmembrane domains with a large hydrophilic loop between the sixth and seventh transmembrane segments (L'Hernault and Arduengo, 1992). SPE-4 is a diverged member of the presenilin (PS) protein family, two members of which are implicated in familial early-onset Alzheimer's disease (Sherrington et al., 1995; Levy-Lahad et al., 1995). The PS 1 and PS 2 mRNAs have been detected throughout the brain and in many non-neuronal tissues (Sherrington et al., 1995; Rogaev et al., 1995; Kovacs et al., 1996). This widespread expression pattern suggests the PS encoded proteins are involved in a ubiquitous cellular function. Indeed, while transgenic mice that are null for mouse PS 1 exhibit gross defects in the central nervous system (Shen et al., 1997; Wong et al., 1997), they also have many anatomical defects, including skeletal abnormalities that presumably contribute to their death as neonates (Shen et al., 1997). Consequently, analyses of those regions conserved between SPE-4 and the other PS family members might provide important clues to their essential cellular function(s).

In this study, we have further characterized *spe-4* mutants to determine the cellular location of its encode protein, SPE-4, and how SPE-4 disrupts the asymmetric partitioning of cellular components during spermatogenesis. Immunofluorescence was employed to examine the distribution of SPE-4 and cytoskeletal proteins subject to asymmetric partitioning during spermatogenesis. We also report the DNA sequences of five *spe-4* point mutations and how these mutants alter the presence and/or pattern of SPE-4 and cytoskeletal proteins during spermatogenesis.

MATERIALS AND METHODS

Strains and genetics

Culture, manipulation of worms, and genetic analyses were performed by standard methods (Brenner, 1974). All strains used in this work, except *spe-4(q347),* were derived from the wild-type *C. elegans* strain var. Bristol N2. Standard *C. elegans* nomenclature has been used throughout this paper (Horvitz et al., 1979). The isolation of *spe-4(q347),* provided by T. Schedl (Washington University School of Medicine, St Louis, MO), *spe-4 (hc78)* and *spe-4 (hc81)* was described previously (L'Hernault et al., 1988; L'Hernault and Arduengo, 1992). The ethyl methane sulfonate induced alleles *spe-4(eb12) and spe-4(eb27)* were obtained through F1 non-complementation to *spe-5(hc110) dpy-5(e61) unc-13(e1091)spe-4(q347)*I. The 178 bp deletion of *spe-4*(*q347)* results in an restriction fragment length polymorphism that is readily identified in worms carrying this mutation (L'Hernault and Arduengo, 1992). Primer set B (Table 1) was used to polymerase chain reaction (PCR) amplify DNA from new candidate *spe-4* alleles, which were confirmed to lack a *spe-4(q347)* associated restriction fragment length polymorphism. The psoralen induced allele *spe-4(tx1)* was the generous gift of Diane Shakes (College of William and Mary, Williamsburg, VA). Genetic markers used were LGI, *unc-13(e51),* and *dpy-5(e61);* LGIV *fem-1(hc17ts)* (Nelson et al., 1978) and *sup-24(st354)* (Kondo et al., 1990); LGV, *him-5(e1490)* (Hodgkin et al., 1979); LGX, *sup-7(st5), sup-21(e1957)* and *sup-28(e2058)* (Kondo et al., 1990). The mutation *sDf5* (Rose and Baillie, 1980) and the reciprocal translocation *szT1* (Fodor and Deak, 1985; McKim et al., 1988) were used to balance and maintain the heterozygous *spe-4* strains used in this study. We recovered approximately 25% homozygous *unc-13* animals from *sDf5*/*spe-4* strains during an amber suppression screen with *sup-21*, *sup-24*, and *sup-28*, suggesting that '*sDf5*' is actually a recessive lethal amber mutation *in cis* to *unc-13*.

PCR and sequencing of *spe-4* mutations

PCR products derived from *spe-4* mutants were directly sequenced using Sequenase version 2.0 (Amersham Life Science, Inc.). L4 hermaphrodite progeny of *spe-4*/+ hermaphrodites were transferred to individual microwells and scored 24 hours later for self-sterility. Sterile worms were picked into a drop of M9 buffer and rinsed in three changes of PCR lysis buffer (50 mM KCl, 10 mM Tris-HCl, pH 8.2, 2.5 mM $MgCl_2$, 0.45% NP-40, 0.45% Tween-20, 0.1 mg/ml gelatin). Worms were frozen at −20°C at a concentration of two worms/μl, and a worm lysate was prepared (Barstead and Waterston, 1991). Three overlapping *spe-4* gene segments were amplified by PCR from 10 μl of worm lysate (approximately two worms/μl) using Taq DNA polymerase (Promega Corp., Madison, WI) with the primer pairs described in Table 1. For each allele, one strand of complete sequence from the coding sequence was obtained, and mutations were confirmed by sequencing both strands.

Fusion protein, peptides and antisera preparation

Only rabbits with preimmune sera that did not show immunoreactivity to *C. elegans* proteins by either immunoblot or immunofluorescence were selected for antisera generation (not shown). One series of rabbits were immunized with a SPE-4 fusion protein that consisted of 115 amino acids from the hydrophilic loop region of SPE-4 (indicated by arrowheads at amino acids 241-356 in Fig. 2A; also see L'Hernault and Arduengo, 1992) fused in-frame to *Schistosoma japonicum* glutathione S-transferase (GST) in the pGEX-2T bacterial expression vector (Smith and Johnson, 1988). *Escherichia coli* BL21 cells containing this construct were grown in liquid culture at 37°C, and SPE-4 fusion protein expression was induced with 0.5 mM isopropyl-β-D-thiolgalactopyranoside. Cells were lysed by rapid freeze-thaw cycles with lysozyme (20 mg/ml) in the presence of leupeptin (1

Table 1. Single stranded DNA primers used for PCR

Primer set	5′ to 3′ sequence	Position in the *spe-4* sequence*
A	ATTACCTGTCTAAAAATGGACAC	1- 23; sense primer
	TTTTTTGAGTGGACCCATCGG	619-653; antisense primer
B	TTTGCCGTTTTAGCACCGATGGG	619-641; sense primer
	TCAGATGTTGACACAGTGGTGCT	1,036-1,058; antisense primer
C	CTGCAGGATCCAATCAAGAAGG	731-753; sense primer
	CGATACTATGTATTCTTTGCC	last 21 nts; antisense primer

*See L'Hernault and Arduengo (1992) for positions in the *spe-4* sequence. Primer set A allows amplification of a 1.1 kb DNA sequence of *spe-4* extending from the transcription start site into exon 4. Primer set B allows amplification of a 0.6 kb DNA sequence of *spe-4* extending from exon 4 into exon 6. Primer set C allows amplification of a 1.0 kb sequence of *spe-4* extending from exon 5 to beyond the polyadenylation site into the 3′ untranslated region.

μg/ml) and aprotinin (20 μg/ml). The bacterial lysate was treated with DNase I and purified over a glutathione affinity column. The fusion protein was checked for absence of degradation by SDS-PAGE and subsequently used to either immunize rabbits or prepare affinity columns. Affinity columns were prepared by covalently coupling protein to a 1:1 mixture of Affigel 10 and Affigel 15 (Bio-Rad Laboratories, Richmond, CA). Antisera were cleared of GST antibodies by passage over a GST affinity column until no GST reactivity was evident on immunoblots. These GST-cleared sera were then affinity purified over a column containing the SPE-4/GST fusion, and bound antibodies were eluted by pH 3.0 glycine treatment directly into 1 M Tris-HCl, pH 8.0, buffer. Affinity purified anti-SPE-4 sera were all used at a 1:10 dilution. All of the SPE-4 antisera prepared in this manner showed staining of sperm and no staining of any somatic tissues (not shown). For some experiments, affinity purified SPE-4 antisera were subsequently preabsorbed to an acetone powder of *fem-1(hc17ts)* worms, which do not make any sperm (Nelson et al., 1978); this treatment had no effect on the specificity of anti-SPE-4 staining (not shown).

A second series of rabbits were immunized with a synthetic peptide that was covalently coupled to carrier protein. A 22mer synthetic peptide that corresponded to residues 355-376 in the deduced SPE-4 polypeptide sequence (positions indicated by arrowheads in Fig. 2A; also see L'Hernault and Arduengo, 1992) was synthesized by the Emory University Microchemical Facility. This peptide had an N-terminal cysteine residue that was used for conjugation to either keyhole limpet hemocynanin (KLH; Sigma Chemical Co., St Louis, MO) or bovine serum albumin (BSA; Sigma) carrier protein. Covalent conjugation was performed with *m*-maleimido-benzoyl-*N*-hydroxysuccinimide as the coupling reagent (Liu et al., 1979) essentially as described previously (Green et al., 1982). The resulting antisera were purified by peptide affinity chromatography on an Affigel 10 and 15 (Bio-Rad Laboratories) column in a manner similar to that described above for fusion protein antisera.

Immunohistochemistry

L4 stage males were placed on agar plates seeded with *E. coli* OP50 (Brenner, 1974) and grown without hermaphrodites for two or three days at 20°C. Three to six males were dissected in 3 μl SM1 plus dextrose (Nelson and Ward, 1980; Machaca et al., 1996) on a slide coated with 2% BSA. The dissected worms were fixed in 4% paraformaldehyde (Electron Microscopy Sciences, Fort Washington, PA) in SM1 plus dextrose in a humid chamber for 30 minutes (Machaca and L'Hernault, 1997). The slides were rinsed in PBS (150 mM NaCl, 16 mM Na_2HPO_4, 4 mM NaH_2PO_4), and unreacted aldehydes were reduced by sodium borohydride ($NaBH_4$; 0.5 mg/ml in PBS). Cells were permeabilized with 0.5% Triton X-100 in PBS for five minutes at room temperature. Primary antibodies were diluted in either PBS containing 1% BSA, 0.5% Triton X-100, 0.05% sodium azide and 1 mM EDTA or PBS containing 5% normal goat serum and incubated with the dissected worms for one or two hours at room temperature. Slides were washed four times for four minutes each time in 5% normal goat serum in PBS and incubated with secondary antibodies for 30 minutes. The slides were then washed in PBS containing 5% normal goat serum and 4,6-diamidino-2-phenylindole (DAPI; 1 μg/ml). Samples were mounted in 1,4-diazabicyclo-[2.2.2] octane (Sigma Chemical Co.) saturated Aquamount (Lerner Laboratories, Pittsburgh, PA).

The cell line that secretes the monoclonal antibody 1CB4 (Okamoto and Thomson 1985) was provided by J. Ahringer and J. Hodgkin, and culture supernatant was prepared by C. Heilman and A. I. Levey (Department of Neurology, Emory University School of Medicine). 1CB4 hybridoma culture supernatant was used for immunofluorescence at a 1:100 dilution. The anti-α-tubulin monoclonal antibody B-5-1-2 was provided as a hybridoma culture supernatant by W. Sale and used at a 1:20 dilution for these studies (Sale et al., 1988). Total actin was visualized using a monoclonal antibody from Sigma Chemical Co. (St Louis, MO) at a dilution of 1:40.

Mouse monoclonal primary antibodies were visualized by using either rhodamine (RITC)-conjugated, affinity purified goat anti-mouse or fluorescein (FITC)-conjugated affinity purified goat anti-mouse IgG secondary antibodies (Jackson ImmunoResearch Laboratories, Inc., West Grove, PA). Polyclonal sera generated in rabbits were detected with a FITC-conjugated affinity purified $F(ab')_2$ fragment of goat anti-rabbit secondary antibody (Sigma). All secondary sera were used a 1:1,000 dilution in PBS containing 5% normal goat serum. All microscopy employed a Zeiss Axioplan microscope fitted with a ×100 Plan Neofluor objective, and micrographs were taken through appropriate filters on Fujichrome color slide film that was processed to E.I. 1600. In Fig. 3, panel A5, DAPI, FITC and RITC were imaged simultaneously with a triple pass filter set (Chroma Technology Corp., Brattleboro, VT). Color slides were converted to digital images that were stored on a Kodak Photo CD, and figures were composed with Adobe PhotoShop 4.0.

RESULTS

Genetic and molecular analysis of *spe-4* alleles

Trans heterozygotes of all possible *spe-4* recessive allele combinations are sterile when mutants are grown at 20°C or 25°C. Complete penetrance for self sterility is observed in *spe-4* homozygotes except for *spe-4(eb27)*, which is a nonsense mutant that produces an average of one offspring per one hundred homozygotes (data not shown). The *spe-4* alleles were sequenced to determine their mutational change, and the results appear in Fig. 2A together with the sequence of *spe-4(q347)* that was reported previously (L'Hernault and Arduengo, 1992). The alleles *hc81* and *eb27* contain amber mutations at amino acid positions 116 (glutamine) and 190 (tryptophan), respectively. The allele *tx1* contains a mutation that changes a tryptophan at position 199 to an opal nonsense mutation. The alleles *hc78* and *eb12* both contain missense mutations. The *hc78* mutation changes a serine to a phenylalanine at position 177. The allele *eb12* is a missense mutation that results in a substitution of a lysine residue for a proline residue at position 440. This proline residue, which is located close to the carboxy terminus, is conserved among ten presenilin family members (Fig. 2B, arrow).

We examined the *spe-4(eb27)* amber mutant in an attempt to determine why it was detectably weaker than the other available mutants (see above). This amber mutant, if it is capable of synthesizing any protein, could allow formation of a less than half-length truncated polypeptide because it contains a premature stop codon at a position that normally encodes a tryptophan. The ability of *spe-4(eb27)* mutants to produce any progeny suggests that a small amount of functional protein is present. In *C. elegans*, the phenotype of amber mutants can frequently be either partially or completely suppressed by tRNA suppressors that insert a tryptophan at the site of an amber codon. Consequently, suppression of the *spe-4(eb27)* amber allele was tested by constructing double mutants with the tRNA amber suppressing mutants *sup-7(st5)X* (Waterston, 1980), *sup-21(e1957)X*, *sup-24(st354) IV* or *sup-28(e2058)X* (Kondo et al., 1990). None of the four *spe-4(eb27)*; *sup* double mutants showed elevated self fertility, indicating that suppression had not occurred. The amber allele *spe-4(hc81)* was previously tested for amber suppression and was not suppressed by *sup-7(st5)* (L'Hernault et al., 1988).

Characterization of SPE-4 polyclonal antisera

Polyclonal sera were generated against either a peptide conjugated to a carrier protein or a fusion protein containing 115 amino acids from the hydrophilic loop of SPE-4 (see Fig. 2A) in-frame to GST. All antisera were affinity purified prior to use in immunofluorescence experiments. The *spe-4(q347)* allele (see Fig. 2A) is a deletion within the hydrophilic loop region that shifts the reading frame and results in a premature stop. Therefore, the *spe-4(q347)* allele contains only four codons from the SPE-4 protein encoding region used to generate the fusion protein antisera and none of the information used to generate the peptide antiserum. Consequently, if these sera are specific for SPE-4 epitopes, they should not recognize any proteins in arrested spermatocytes from animals homozygous for the *spe-4(q347)* mutation.

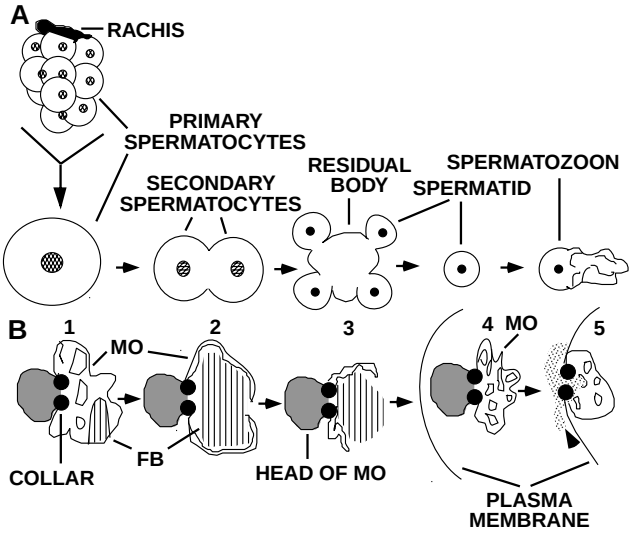

Fig. 1. Summary of wild-type spermatogenesis (A) and morphogenesis of the fibrous-body-membranous organelle (FB-MO) complexes (B). (A) Primary spermatocytes develop in syncitium with a central core of cytoplasm named the rachis from which they bud after initiating meiosis. A primary spermatocyte divides into two secondary spermatocytes. Cytoplasmic and membrane components not required for further development are segregated into the residual body during spermatid budding. Spermatids bud from the residual body as nonmotile cells with no obvious cellular polarity. Spermatids activate into spermatozoa with a single, motile pseudopod that imparts polarity to the cell. (B) The fibrous body (FB) develops in close association with the double layered membrane of the membranous organelles (MO); (B2) the FBs are completely surrounded by the MO membrane in the primary spermatocyte. The MOs are separated by an electron-dense collar into a head region and a body that contains the major sperm protein (MSP) fibers within the FB. The FB-MO complexes are formed by the time primary spermatocytes bud off the rachis; (B3) when the spermatid forms and buds from the residual body, the membranes surrounding the fibrous bodies begin to retract, and the MSP fibers depolymerize and the constituent dimers disperse; (B4) the MOs, which now lack FBs, localize near the spermatid plasma membrane; (B5) the head of the MO fuses with the plasma membrane upon spermatid activation and its contents exocytose onto the cell surface (arrowhead). A permanent fusion pore remains in the plasma membrane of the spermatozoon at the point of each MO fusion. Each cell contains several dozen MOs. Note that the spermatogenesis pathway depicted in A is not drawn to the same scale as the FB-MO morphogenesis in B.

Prior work revealed that FB-MO development was abnormal in *spe-4* mutants, and one possible explanation was that SPE-4 might reside in the FB-MO membranes (L'Hernault and Arduengo, 1992). This cellular compartment is labeled specifically by the monoclonal antibody 1CB4 (Okamoto and Thomson, 1985), so a coincident immunofluorescent signal from 1CB4 and SPE-4 specific antibodies would indicate that SPE-4 also localizes to the FB-MOs. Furthermore, since we show that 1CB4 stains the aberrant FB-MOs found in *spe-4* mutant cells (see below), it serves as a positive control in immunofluorescence experiments.

FB-MOs partition to spermatids as they bud from the residual body during wild-type spermatogenesis, and this partitioning is revealed by the MO specific antibody 1CB4 (Fig. 3A3). Representative SPE-4 staining during spermatid formation is shown for the peptide antiserum EU43 (Fig. 3A4). These two antisera exhibit an apparently coincident signal, suggesting that SPE-4 resides in the FB-MOs (Fig. 3A5). SPE-4 also localizes within the spermatozoon cell body as revealed by staining with the fusion protein antiserum 9910 (Fig. 3B4) and appears to show dim staining of the pseudopod. This SPE-4 signal in the spermatozoon, including a dim signal from the pseudopod, coincides with 1CB4 staining (Fig. 3B3); similar results are observed with other SPE-4 sera (data not shown). Prior work showed that 1CB4 localizes specifically to the MOs by immunogold electron microscopic analysis, perhaps indicating that the signal associated with the pseudopod is nonspecific (Okamoto and Thomson, 1985). Affinity purified 9910 serum fails to recognize any epitope in *spe-4(q347)* cells, showing that it is specific for SPE-4 epitopes (Fig. 3C4). The *spe-4(hc78)* allele, which has a null phenotype, is a missense mutation in which a serine residue is replaced by a phenylalanine residue (see Fig. 2). Immunolocalization of SPE-4 in *spe-4*(*hc78)* arrested spermatocytes reveals that the mutant protein is synthesized and detectable at low levels in arrested spermatocytes (Fig. 3D4). The missense *spe-4(eb12)* allele, which also has a null phenotype, results in the substitution of a leucine residue for a proline residue near the C terminus (Fig. 2). Unlike the *spe-4(hc78)* mutation, *spe-4(eb12)* is within a motif that is present in ten presenilin family members (Levitan and Greenwald, 1995; Levy-Lahad et al., 1995; Rogaev et al., 1995; Sherrington et al., 1995; Hong and Koo, 1997; Li and Greenwald, 1997; Tsujimura et al., 1997; see Fig. 2B). Terminal *spe-4(eb12*) spermatocytes were stained with affinity purified 9910 antisera, and this revealed a punctate SPE-4 signal (Fig. 3E4) that coincided with the 1CB4 FB-MO signal (Fig. 3E3). These data indicate that, even though *spe-4(eb12)* mutants can both synthesize mutant SPE-4 and localize it within the appropriate subcellular compartment, the mutational defect prevents subsequent sperm morphogenesis.

The fusion protein antiserum EU20 stains wild-type cells in a punctate manner (Fig. 3F4) that is similar to that observed for 9910 (Fig. 3B4). However, this antiserum also recognizes an epitope in *spe-4(q347)* null cells (Fig. 3G4). Similar results were obtained for affinity purified EU21 antiserum (data not shown). Staining with all SPE-4 antisera on whole male worm carcasses is restricted to the gonad of the worm (data not shown). All four SPE-4/GST fusion antisera (9910, 9911, EU20 and EU21) and antisera to two different peptides (EU43 and 11950) give a punctate signal that co-localizes with the 1CB4 signal and never stains the plasma membrane.

spe-4 mutants aberrantly localize tubulin

The FB-MOs are not the only cellular component to exhibit asymmetric partitioning as spermatids bud from the residual body during *C. elegans* spermatogenesis. Consequently, *spe-4* mutants were examined for defects in segregating other (non FB-MO) cellular components during spermatid budding.

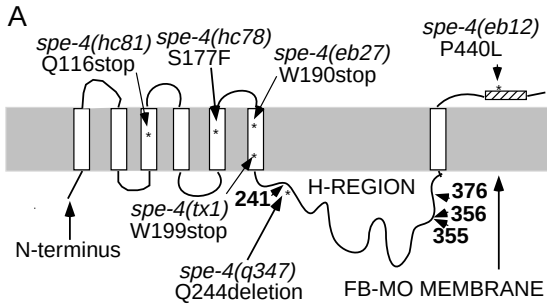

B

C. elegans SPE-4	435	EESTT**PALP**LPVICGTFCY**F**
C. elegans SEL-12	405	FKRAL**PALP**ISIFSGLIFY**F**
C. elegans HOP-1	319	SQTAL**PALP**FPLAIAAIFY**F**
Drosophila	489	WRKAL**PALP**ISITFGLIFC**F**
Xenopus α or β	394	FKKAL**PALP**ISITFGLIFY**F**
Rat PS1	429	FKKAL**PALP**ISITFGLIFY**F**
Mouse PS1	428	FKKAL**PALP**ISITFGLVFY**F**
Human PS1	428	FKKAL**PALP**ISITFGLVFY**F**
Human PS2	418	FKKAL**PALP**ISITFGLIFY**F**
Arabidopsis	414	YNRAL**PALP**ISIMLGVVFY**F**

Fig. 2. The location of SPE-4 mutations. (A) Proposed topology of SPE-4 within the FB-MO membrane, and the positions of six mutations are indicated by asterisks. This membrane topology was derived using the Kyte and Doolittle (1982) algorithm set at a window of 19 residues. Membrane spanning regions are indicated by white rectangular boxes. SPE-4 is predicted by this algorithm to have seven membrane spanning domains (L'Hernault and Arduengo, 1992). The small striped box near the C terminus is a highly hydrophobic region that might be able to span the membrane bilayer; it is just below significance using the above-stated algorithm parameters. Amino acid positions of the mutations are indicated by numbers. The mutation *spe-4(hc81)* changes the glutamine at position 116 to a stop codon; the *spe-4(hc78)* mutation changes a serine residue to a phenylalanine residue at position 177; the mutations *spe-4(eb27)* and *spe-4(tx-1)* convert tryptophan residues to stop codons at positions 190 and 199, respectively; the previously described *spe-4(q347)* mutation (L'Hernault and Arduengo, 1992) is a 178 base pair deletion affecting positions 244-299 and portions of intron five creating multiple stop codons 3′ to the deletion; the *spe-4(eb12)* mutation results in the substitution of a leucine residue for a proline. H-REGION is the hydrophilic polypeptide region that contains the two amino acid sequences (indicated by arrowheads) used to raise the antisera described in the paper. Amino acid residues 241-356 were expressed as a fusion protein in bacteria and used to generate the polyclonal antisera 9910, 9911 and EU20. A synthetic peptide corresponding to amino acid residues 355-376 was used to generate the polyclonal antisera EU 43 (see Materials and Methods); (B) Alignment of conserved C-terminal portions of the presenilin family members. The conserved PALPX(S/P)XXX(G/A)XX(F/C)(Y/C)F motif is highlighted in bold. The first proline of this motif is mutated in *spe-4(eb12)* to a leucine residue. *C. elegans* HOP-1, Li and Greenwald (1997); *C. elegans* SEL-12, Levitan and Greenwald (1995); *C. elegans* SPE-4, L'Hernault and Arduengo (1992); *Drosophila*, Hong and Koo (1997); *Xenopus*, Tsujimura et al. (1997); rat, Taniguchi et al. (1997); human and mouse PS1, Sherrington et al. (1995); human PS2; Levy-Lahad et al. (1995), Rogaev et al. (1995) and *Arabidopsis* (GenBank accession number AC003981).

During wild-type spermatogenesis, nearly all tubulin and actin segregate to the residual body during spermatid budding; most tubulin is deposited in the residual body as part of the meiotic spindle apparatus (Ward, 1986). While *spe-4* mutants complete the second meiotic division and form haploid nuclei, they do not bud spermatids or form a normal residual body (L'Hernault et al., 1988; L'Hernault and Arduengo, 1992). Consequently, we examined *spe-4* mutants for abnormalities in the distribution of actin and tubulin after haploid nuclei were evident.

As previously reported, tubulin localizes within the meiotic spindle apparatus during the early stages of wild-type residual body during formation (Fig. 4A3; Ward, 1986). This spindle is placed in the residual body following completion of the second meiotic division (Fig. 4B3). Budded spermatids lack detectable tubulin under these fixation and photographic exposure conditions, although prior ultrastructural studies shows they have a centrosome (Fig. 4C4; Wolf et al., 1978; Ward et al., 1981). In the *spe-4(hc81)* mutant, the spindle apparatus apparently forms (Fig. 4E3) and functions correctly because karyokinesis is completed and four haploid nuclei are evident (Fig. 4E2). Similar phenomena were observed for other *spe-4* mutants (data not shown). Panel 4F1 shows a Nomarski image of an arrested *spe-4(hc81)* cell at a slightly later developmental stage. This cell has four haploid nuclei (Fig. 4F2), but the two meiotic spindles have disassembled, and their constituent tubulin has accumulated as an unusual layer near the plasma membrane. Similar phenomena are observed in the *spe-4* mutants *hc78* (Fig. 4G3), *eb12* (Fig. 4H3) and *q347* (Fig 4D3). The *spe-4* mutant *eb12* (P440L, see Fig. 2B) occasionally appears to accumulate tubulin in the central region of the cell, perhaps during an unsuccessful attempt to form a residual body (not shown). The aberrant aggregation of tubulin near the plasma membrane of *spe-4* mutant spermatocytes is not observed during wild-type spermatogenesis.

At least one other cytoskeletal protein does not show aberrant accumulation in *spe-4* mutants. Actin staining localizes within the cleavage furrow in *spe-4* cells during cytokinesis of primary spermatocytes, just as in wild type (Nelson et al., 1982; data not shown). Actin shows a distribution that is similar to tubulin and, consistent with prior observations (Ward et al., 1981), does not accumulate at the site of spermatid budding from the residual body; the actin distribution is similar to that shown by tubulin (Fig. 4A3 and 4A4). Actin, like tubulin, is segregated into the residual body as spermatids bud from this structure during wild-type spermatogenesis (Fig. 4B4; Ward, 1986). Terminally arrested *spe-4(q347)* cells contain diffuse actin that does not form obvious aggregations when visualized by immunofluorescence (Fig. 4G4) and this is true for all other examined *spe-4* mutants (data not shown).

DISCUSSION

SPE-4 localizes within the Golgi/ER derived FB-MOs and segregates to spermatids as they bud from the residual body during *C. elegans* spermatogenesis. This suggests that a lack of wild-type SPE-4 in the FB-MOs of *spe-4* mutants probably causes the previously described ultrastructural defects (L'Hernault and Arduengo, 1992). The sequence of five *spe-4*

point mutations was determined, and genetic and cytological techniques were used to further characterize *spe-4* arrested spermatocytes. Three recessive mutations are nonsense and, presumably, cause premature polypeptide chain termination. Two mutations are missense, and one changes a residue found in all members of the presenilin protein family, while the other affects a residue that is unique to SPE-4. Both missense mutants synthesize detectable SPE-4 protein that localizes within the FB-MOs. Tubulin, which is a non FB-MO cytoplasmic component, also exhibits partitioning defects in *spe-4* terminally arrested spermatocytes because it aggregates as an unusual layer near the plasma membrane.

All six described *spe-4* alleles are loss of function, and two of these are amber point mutations. Neither the *spe-4(eb27)* nor the *spe-4*(*hc81)* amber mutants (L'Hernault et al., 1988) exhibit elevated self-fertility (suppression) when tested with the *sup-*

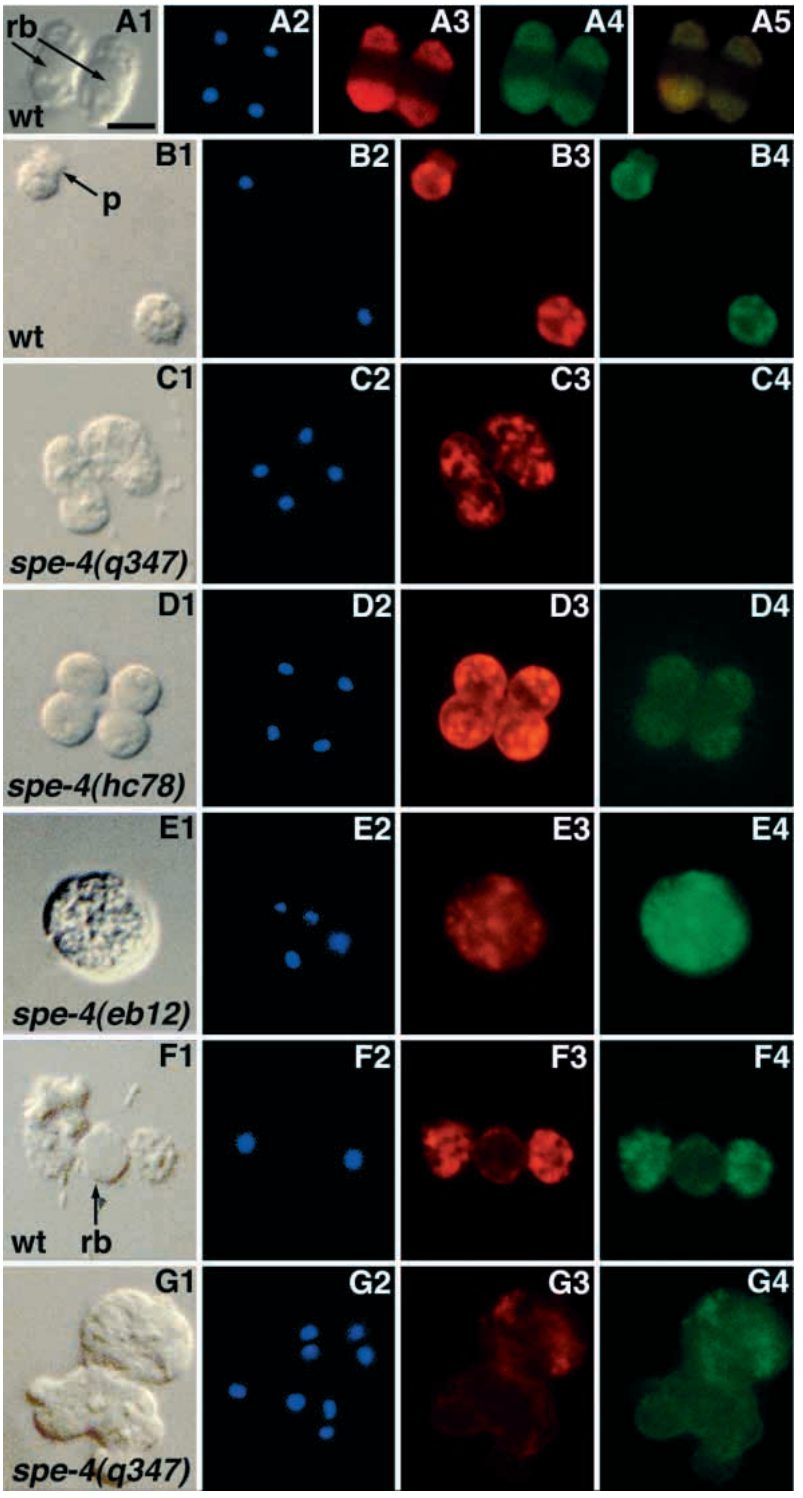

Fig. 3. Immunofluorescence localization of SPE-4 in sperm cells. Bar in A1, 5 μm, applies to all panels. Each horizontal, lettered row contains a series of four or five corresponding images: Nomarski DIC to visualize cytology (#1 panel), DAPI staining to visualize nuclei (blue #2 panel), monoclonal antibody ICB4 staining to visualize the fibrous body-membranous organelle (FB-MO) complexes (RITC red #3 panel), affinity purified anti SPE-4 rabbit polyclonal antibody staining (FITC green #4 panel) and a photograph through a filter set that simultaneously passes the DAPI, RITC and FITC signals (yellow #5). The genotype of the cells depicted in each row is indicated at the bottom of the leftmost panel. All #4 panels were photographed and printed at the same exposure index except that E4 was printed at 50% exposure index relative to the other panels (see below). (A) Wild-type spermatids budding from the residual body (rb). Both 1CB4 staining (A3) and EU43 SPE-4 peptide antiserum staining (A4) occur in spermatids during their budding from the rb and these signals coincide to produce the yellow signal observed in A5. (B) A wild-type spermatid (lower right corner) and a spermatozoon with a single pseudopod (p at arrow) extending from its cell body. Staining with 1CB4 (B3) reveals that the punctate signal is mostly found in the cell body and a similar, overlapping signal (B4) is observed after staining with the 9910 SPE-4 antiserum. (C) *spe-4(q347)* null mutant arrested spermatocyte. Staining with 9910 SPE-4 fusion protein antiserum reveals that no SPE-4 protein is present, as for 9911 SPE-4 antiserum (which was also raised to the same fusion protein and is not shown for wild type). (D) *spe-4(hc78)* mutant arrested spermatocyte. Staining with 9911 SPE-4 antiserum (D4) reveals that this *spe-4(hc78)* missense mutant synthesizes a small amount of mutant SPE-4. (E) *spe-4(eb12)* mutant arrested spermatocyte. Staining with 9910 SPE-4 antiserum (E4) reveals that the *spe-4(eb12)* missense mutant synthesizes a large amount of mutant SPE-4; this panel was printed at 50% of the exposure index relative to the other #4 panels in order to eliminate color over-saturation (compare to B4 and C4). (F) Wild-type spermatids budding from the rb. Staining with the EU20 SPE-4 antiserum (F4) shows segregation of SPE-4 (and probably at least one other protein; see the text for details) to spermatids during development. (G) Two *spe-4(q347)* null mutant spermatocytes. Staining with the EU20 SPE-4 antiserum (G4) reveals a fluorescent signal in this null mutant, suggesting this antiserum recognizes an epitope on a protein other than *spe-4* (for further explanation, see the text).

7(st5) amber suppressor. The amber suppressors *sup-21(e1957)*, *sup-24(st354)* and *sup-28(e2058)* were also not able to suppress *spe-4(eb27)*. These suppressors are known to be expressed in the germline (Kondo et al., 1990) and all insert tryptophan, which is the amino acid residue normally located at the position of the *spe-4(eb27)* premature stop codon. The only previously described amber suppression within the male germline is weak suppression of ~2% of *spe-26(hc139ts)* homozygotes by *sup-7* carried on a transgene (Varkey et al., 1995). Perhaps the multiple copies of *sup-7* present on this

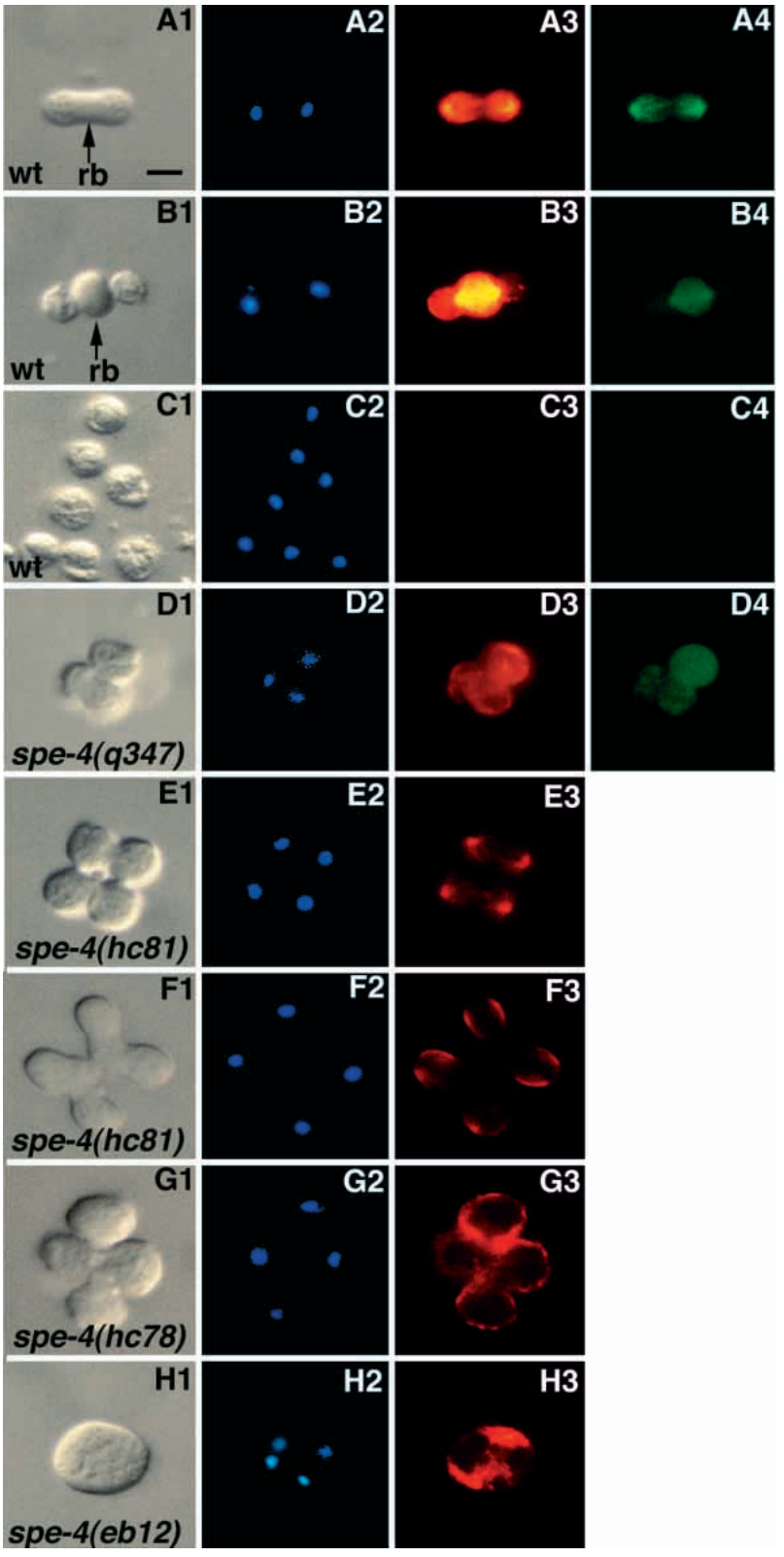

Fig. 4. Immunofluorescence localization of tubulin and actin in sperm. Bar in A1, 5 μm, applies to all panels. Each horizontal, lettered row contains a series of either three or four corresponding images: Nomarski DIC to visualize cytology (#1 panel), DAPI staining to visualize nuclei (blue #2 panel), anti-α-tubulin monoclonal antibody staining to visualize unpolymerized tubulin and microtubules (red #3 panel) and anti-actin rabbit polyclonal antibody staining to reveal both G and F actin (green #4 panel). The genotype of the cells depicted in each row is indicated at the bottom of the leftmost panel. (A) Wild-type spermatids beginning to form a residual body (rb) during completion of the second meiotic division. Anti tubulin staining (A3) reveals a well formed meiotic spindle. Anti actin staining (A4) reveals a pattern that is similar to the microtubules of the meiotic spindle. (B) Wild-type spermatids budding from a rb. Anti tubulin staining (B3) reveals that most tubulin is segregated into the rb after karyokinesis is complete. Anti-actin staining (B4) reveals that actin also segregates into the rb after karyokinesis is complete. (C) A field of seven spermatids reveals that they do not contain detectable tubulin (C3) or actin (C4); the centrioles are not visible in these photographs. (D) A *spe-4(q347)* null mutant spermatocyte that has arrested without forming a rb. Karyokinesis has been completed (D2) and the arrested spermatocyte contains four condensed nuclei, but only three are visible in this image. Anti-tubulin staining (D3) reveals that some of the tubulin is associated with the plasma membrane in this *spe-4(q347)* null mutant spermatocyte. Anti-actin staining (D4) reveals that actin does not appear to form any unusual structures or aggregations in this *spe-4(q347)* null mutant arrested spermatocyte. (E) A *spe-4(hc81)* mutant spermatocyte that is attempting cell division. Staining with anti-tubulin antibodies (E3) reveals the spindle apparatus is well formed in these cells. (F) Another *spe-4(hc81)* mutant spermatocyte at a later stage than the cell shown in E. This cell has arrested after forming a small, anuclear structure that is reminiscent of a residual body. Anti-tubulin staining (F3) shows that the spindle has disassembled and the tubulin is now associated with the plasma membrane in a aberrant manner. (G) A *spe-4(hc78)* mutant spermatocyte that has arrested without forming a residual body. Anti-tubulin staining (G3) shows that the spindle has disassembled and the tubulin is associated with the plasma membrane in a aberrant manner. (H) A *spe-4(eb12)* mutant spermatocyte that has arrested without attempting to form spermatid-like cells. Karyokinesis has been completed (H2) because four condensed nuclei are present, and tubulin accumulates as discrete aggregates (H3) in several locations.

transgene (Mello et al., 1991) allow expression during spermatogenesis that is sufficient for weak suppression.

Both the *spe-4(eb27)* amber and the *spe-4(tx1)* opal alleles are nonsense mutations located within putative transmembrane region 6. Like most *spe-4* mutants, *spe-4(tx1)* is completely self-sterile. In contrast, *spe-4(eb27)* mutant produces about one progeny per 100 examined homozygous hermaphrodites and is the weakest *spe-4* mutant with respect to self-fertility. Perhaps a mechanism exists in the testes that permits natural amber suppression but does not allow opal suppression. This read through mechanism presumably involves base wobble (Crick, 1966) and why its effects are limited to one amber mutation is not clear. At this time, it is not known why *spe-4(eb27)* is the weakest *spe-4* mutant.

The MOs of nematode sperm begin development prior to the budding of the primary spermatocyte from the rachis, appearing first as an enlargement of a Golgi vesicle that is surrounded by a cup-shaped cisterna of endoplasmic reticulum (Wolf et al., 1978). The localization of SPE-4 to the FB-MOs is intriguing because two human presenilin family members (PS-1 and PS-2) are localized to the Golgi apparatus and endoplasmic reticulum in transfected COS cells, H4 human neuroglioma cells and primate brain (Kovacs et al., 1996; Doan et al., 1996; DeStrooper et al., 1997; Lah et al., 1997). The fact that SPE-4 and the human presenilins share a common subcellular localization suggests that they may serve similar roles in cell function.

Two affinity purified fusion antisera (EU20 and EU21) that stain MOs and only recognized male gonadal epitopes also recognized epitope(s) in *spe-4(q347)* mutant spermatocytes. SPE-4 apparently shares an epitope with at least one other sperm specific protein. A similar phenomenon has been observed previously for a monoclonal antibody that recognizes at least eight different *C elegans* sperm proteins on immunoblots (Ward et al., 1986). The dominant epitope recognized by the SPE-4 antisera EU20 and EU21 might represent a conserved signal that is characteristic of certain protein(s) that reside within the Golgi/ER derived MO vesicle. Alternatively, a second sperm specific homologue of SPE-4 might exist. The most significant SPE-4 homologies (E value of less than 1e-07) detected in BLAST 2.0.5 searches (Altschul et al., 1997) are to the other presenilins, including *C. elegans* SEL-12 (Levitan and Greenwald, 1995) and HOP-1 (Li and Greenwald, 1997). No other significant homologies, including within the available *C. elegans* genome sequence, were detected in these searches. Since the antisera EU20 and EU21 show testes specific localization by immunofluorescence, this suggests they recognize a protein(s) other than either HOP-1 or SEL-12 because these two presenilin homologs affect many somatic cell types.

There are no conserved motifs present in the presenilin protein sequences to suggest the probable biochemical function of these proteins. However, all known presenilin family members contain a PALPX(S/P)XXX(G/A)XX(F/C)(Y/C)F amino acid motif near their C terminus, suggesting that this region is functionally significant (The Xs are also strongly conserved among family members. For instance, there are no charged residues in this region in any family member). The first proline of this PALP motif is changed to a leucine in the *spe-4(eb12)* missense mutant (Fig. 2B). This residue is necessary for the function but not for synthesis or localization because *spe-4(eb12)* encoded SPE-4 is observed within FB-MOs. Searches of SWISS-PROT with this motif reveals that it is unique to the presenilins and their homologs. Understanding how this mutation affects the function of SPE-4 should reveal the role this region plays within the presenilin protein family. Similar immunofluorescent results were obtained for the *spe-4(hc78)* mutation, which affects an amino acid residue unique to SPE-4.

So far, only recessive loss of function mutations in *spe-4* have been obtained (L'Hernault et al., 1988; L'Hernault and Arduengo, 1992). In contrast, mutations in the presenilin genes that cause familial Alzheimer's disease (FAD; 41 mutations described for PS1 and two for PS2; reviewed by Hardy, 1997) present as dominant mutations. Several dominant PS1 and PS2 mutants are associated with enhanced secretion of β-amyloid in human serum (Scheuner et al., 1996), cultured mammalian cells (Martins et al., 1995; Tomita et al., 1997) and transgenic mice (Borchelt et al., 1996), consistent with a role for the mammalian presenilins in intracellular protein trafficking. In contrast, secretion of β-amyloid is reduced in loss of function PS1 mutants because proteolytic processing of the amyloid precursor protein is inhibited (De Strooper et al., 1998). If dominant mutations in *C. elegans spe-4* can be recovered, it would be interesting to compare them to existing recessive mutants for secretory or other membrane trafficking defects.

Defects in tubulin localization were observed during spermatogenesis in *spe-4* mutants. Normally, tubulin and actin are segregated into the residual body as spermatids bud from this structure. Most tubulin segregates to the residual body within the meiotic spindle, which stays intact for a period of time after chromosomal segregation (Ward, 1986). Although spermatid budding from the residual body does not occur in terminal *spe-4* spermatocytes, one might expect actin and tubulin to accumulate in the center of the arrested cell (where the residual body would be located in wild-type cells, see Fig. 1A) or perhaps, be distributed diffusely within the cytoplasm. Initially, tubulin forms a functional spindle apparatus in *spe-4* spermatocytes because the nuclear events of meiosis occur and haploid nuclei are observed (L'Hernault and Arduengo, 1992). While actin is distributed diffusely within the cytoplasm of arrested *spe-4* spermatocytes, tubulin aberrantly accumulates in close proximity to the plasma membrane. Studies in the parasitic nematode *Ascaris* have shown that the FB-MOs are associated with the spindle poles during meiosis, perhaps via microtubules (T. Roberts, personal communication). This membrane/spindle pole microtubule affinity could be the mechanism that polarizes the budding of spermatids from the residual body, ensuring that FB-MOs end up in spermatids and the meiotic spindle partitions to the residual body. Perhaps the abnormal FB-MOs present within *spe-4* arrested spermatocytes prevent this association with the meiotic spindle, arrest spermatid budding and cause tubulin to show affinity for non FB-MO membranes. While tubulin is generally thought to be a cytosolic protein, several cases of its association with membranes have been observed (reviewed by Stephens, 1986).

Aberrant positioning of cytoskeletal proteins during spermatogenesis has also been observed in two other *C. elegans spe* mutants. Actin does not show any unusual localization within *spe-5* arrested spermatocytes, and it is distributed diffusely within the cytoplasm in a manner that is

similar to *spe-4* terminal spermatocytes. Tubulin can segregate with nuclei into arrested *spe-5* spermatocytes but it sometimes partitions properly to the residual body in this variable mutant. However, tubulin within *spe-5* spermatocytes never exhibits the type of membrane association apparent in *spe-4* mutant cells (Machaca and L'Hernault, 1997). The *spe-26* gene encodes a protein with homology to previously characterized actin binding proteins. Not surprisingly, the *spe-26* mutant, unlike *spe-4* or *spe-5*, forms unusual accumulations of actin filaments under the plasma membrane in its terminal spermatocytes. The second meiotic spindle remains assembled and persists within the terminal spermatocyte stage that accumulates in *spe-26* mutants (Varkey et al., 1995). These results show that arrest as a *spe-4*-like terminal spermatocyte can be followed by a persistent, stable meiotic spindle (as occur in *spe-26* mutants) and severe defects in FB-MOs (as occur in *spe-5* mutants) do not necessarily cause tubulin to show strange accumulation near the plasma membrane.

Several other mutants arrest spermatogenesis as primary spermatocytes with multiple nuclei, including *spe-7(mn252)* (Sigurdson et al., 1984; Shakes, 1988), *spe-10* (Shakes and Ward, 1989), *spe-5* (L'Hernault et al., 1988; Machaca and L'Hernault, 1997) and *spe-26* (Varkey et al., 1995). These mutants might affect other steps in the same cellular pathway as SPE-4, and analysis of double mutants with *spe-4* may provide further clues to SPE-4 and presenilin function. Recovery of extragenic suppressors might also reveal other molecules operative within the same pathway as SPE-4. Since both the *spe-4(hc78)* and the *spe-4(eb12)* mutations appear to affect function but not localization or synthesis of SPE-4, they might be good candidates for recovery of such suppressors.

Our results permit a model of how SPE-4 functions during spermatogenesis. Clearly, wild-type SPE-4 is required within the FB-MO for the normal morphogenesis and function of this organelle. Disruption of FB-MO morphogenesis in *spe-4* mutants causes these organelles to be scattered througout the cell and not assume a proper position at the poles of the meiotic spindle. This leads to failure of spermatid budding because, apparently, the residual body can form properly only when FB-MOs are localized in the region of the developing spermatid. There is no coordinated way to discard the spindle in the absence of a residual body, and it disassembles into its constituent tubulin that becomes associated with the cell periphery.

We thank D. Shakes for *spe-4(tx1)*, J. Hodgkin, J. Ahringer, C. Heilman, A. Levey and W. Sale for antibodies, Sam Ward, Barry Yedvobnick, Hilary Ellis, Harish Joshi, Doug Eaton, Win Sale and Grant MacGregor and L'Hernault lab members for advice, and Kristie Butze-Mercer for technical support. P. M. Arduengo thanks Frank Berneisen for photographic assistance and the Morningside College Biology faculty for encouragement and meaningful discussions. This work was supported by grants from the NIH (GM40697) and the Emory University Research Committee to S. W. L'Hernault. P. M. Arduengo was partly supported by an NIH Training Grant awarded to Emory University. Some of the stocks used in this work were obtained from the *Caenorhabditis* Genetics Center, which is funded by the NIH National Center for Research Resources.

REFERENCES

Altschul, S. F., Madden, T. L., Schaffer, A. A., Zhang, J., Zhang, Z., Miller, W. and Lipman, D. J. (1997). Gapped BLAST and PSI-BLAST: a new generation of protein database search programs. *Nucl. Acids Res.* **25**, 3389-3402.

Barstead, R. and Waterston, R. H. (1991). Vinculin is essential for muscle function in the nematode. *J. Cell Biol.* **114**, 715-724.

Borchelt, D. R., Thinakaran, G., Eckman, C. B., Lee, M. K., Davenport, F., Ratovitsky, T., Prada, C.-M., Kim, G., Seekins, S., Yager, D., et al. (1996). Familial Alzheimer's disease-linked presenilin 1 variants elevate Aβ1-42/1-40 ratio *in vitro* and *in vivo*. *Neuron* **17**, 1005-1013.

Brenner, S. (1974). The genetics of *Caenorhabditis elegans*. *Genetics* **77**, 71-94.

Crick, F. H. C. (1966). Codon-anticodon pairing: the wobble hypothesis. *J. Mol. Biol.* **19**, 548-555.

DeStrooper, B., Beullens, M., Contreras, B., Levesque, L., Craessaerts, K., Cordell, B., Moechars, D., Bollen, M., Fraser, P., St George-Hyslop, P. and Leuven, F. V. (1997). Phosphorylation, subcellular localization, and membrane orientation of the Alzheimer's disease-associated presenilins. *J. Biol. Chem.* **272**, 3590-3598.

DeStrooper, B., Saftig, P., Craessaerts, K., Vandersticheles, H., Guhde, G., Annaert, W., Von Figura, K. and Leuven, F. V. (1998). Deficiency of presenilin-1 inhibits the normal cleavage of amyloid precursor protein. *Nature* **391**, 387-390.

Doan, A., Thinakaran, G., Brochelt, D. A., Slunt, H., Ratovitskty, H, T., Podlisny, M., Selkoe, D. J., Price, D. L. and Sisodia, S. S. (1996). Protein topology of presenilin 1. *Neuron* **17**, 1023-1030.

Fodor, A. and Deak, P. (1985). The isolation and genetic analysis of a *Caenorhabditis elegans* translocation (*szT1*) strain bearing an X-chromosome balancer. *J. Genet.* **64**, 143-157.

Green, N., Alexander, H., Olson, A., Alexander, S., Shinnick, T. M., Sutcliffe, J. G. and Lerner, R. A. (1982). Immunogenic structure of the influenza virus hemagglutinin. *Cell* **28**, 477-487.

Hardy, J. (1997). Amyloid, the presenilins and Alzheimer's disease. *Trends Neurosci.* **20**, 154-159.

Hodgkin, J., Brenner, S. and Horvitz, H. R. (1979). Nondisjunction mutants of the nematode *Caenorhabditis elegans*. *Genetics* **91**, 67-94.

Hong, C. and Koo, E. H. (1997). Isolation and characterization of *Drosophila* presenilin homolog. *NeuroReport* **8**, 665-668.

Horvitz, H. R., Brenner, S., Hodgkin, J. and Herman, R. K. (1979). A uniform genetic nomenclature for the nematode *Caenorhabditis elegans*. *Mol. Gen. Genet.* **175**, 129-133.

Klass, M. R. and Hirsh, D. (1981). Sperm isolation and biochemical analysis of the major sperm protein from *Caenorhabditis elegans*. *Dev. Biol.* **84**, 299-312.

Kondo, K., Makovec, B., Waterston, R. H. and Hodgkin, J. (1990). Genetic and molecular analysis of eight $tRNA^{Trp}$ amber suppressors in *Caenorhabditis elegans*. *J. Mol. Biol.* **215**, 7-19.

Kovacs, D. M., Fausett, H. J., Page, K. J., Kim, T., Moir, R. D., Merriam, D. E., Hollister, R. D., Hallmark, O. G., Mancini, R., Felsenstein, K. M., Hyman, B. T., Tanzi, R. E. and Wasco, W. (1996). Alzheimer-associated presenilins 1 and 2: neuronal expression in brain and localization to intracellular membranes in mammalian cells. *Nature Med.* **2**, 224-229.

Kyte, J. and Doolittle R. F. (1982). A simple method for displaying the hydropathic character of a protein. *J. Mol. Biol.* **157**, 105-132.

Lah, J. J., Heilman, C. J., Nash, N. R., Rees, H. D., Yi, H., Counts, S. E. and Levey, A. I. (1997). Light and electron microscopic localization of presenilin-1 in primate brain. *J. Neurosci.* **17**, 1971-1980.

Levitan, D. and Greenwald, I. (1995). Facilitation of *lin-12*-mediated signaling by *sel-12*, a *Caenorhabditis elegans* S182 Alzheimer's disease gene. *Nature* **377**, 351-354.

Levy-Lahad, E., Wasco, W., Poorkaj, P., Romano, D. M., Oshima, J., Pettingell, W. H., Yu, C., Jondro, P. D., Schmidt, S. D., Wang, K., et al. (1995). Candidate gene for the chromosome 1 familial Alzheimer's disease locus. *Science* **269**, 973-977.

L'Hernault, S. W., Shakes, D. C. and Ward, S. (1988). Developmental genetics of chromosome I spermatogenesis-defective mutants in the nematode *Caenorhabditis elegans*. *Genetics* **120**, 435-452.

L'Hernault, S. W. and Arduengo, P. M. (1992). Mutation of a putative sperm membrane protein in *Caenorhabditis elegans* prevents sperm differentiation but not its associated meiotic division. *J. Cell Biol.* **119**, 55-68.

L'Hernault, S. W. (1997). Spermatogenesis. In *C. elegans* II (ed. D. L. Riddle,

T. Blumenthal, B. J. Meyer and J. R. Priess), pp. 274-294. Cold Spring Harbor Laboratory Press, New York

Li, X. and Greenwald, I. (1997). HOP-1, a *Caenorhabditis elegans* presenilin, appears to be functionally redundant with SEL-12 presenilin and to facilitate LIN-12 and GLP-1 signaling. *Proc. Nat. Acad. Sci. USA* **94**, 12204-12209.

Liu, F.-T., Zinnecker, M., Hamaoka, T. and Katz, D. H. (1979). New procedures for preparation and isolation of conjugates of proteins and a synthetic copolymer of D-amino acids and immunological characterization of such conjugates. *Biochemistry* **18**, 690-697.

Machaca, K., DeFelice, L. J. and L'Hernault, S. W. (1996). A novel chloride channel localizes to *Caenorhabditis elegans* spermatids and chloride channel blockers induce spermatid differentiation. *Dev. Biol.* **176**, 1-16.

Machaca, K. and L'Hernault, S. W. (1997). The *Caenorhabditis elegans spe-5* gene is required for morphogenesis of a sperm specific organelle and is associated with an inherent cold-sensitive phenotype. *Genetics* **146**, 567-581.

Martins, R. N., Turner, B. A., Carroll, R. T., Sweeney, D., Kim, K. S., Wisniewski, H. M., Blass, J. P., Gibson G. E. and Gandy, S. (1995). High levels of amyloid-β protein from S182 (Glu^{246}) familial Alzheimer's cells. *NeuroReport* **7**, 217-220.

McKim, K. S., Howell, A. M. and Rose, A. M. (1988). The effects of translocations on recombination frequency in *Caenorhabditis elegans*. *Genetics* **120**, 987-1001.

Mello, C. C., Kramer J. M., Stinchcomb, D. and Ambros, V. (1991). Efficient gene transfer in *C. elegans*: extrachromosomal maintenance and integration of transforming sequences. *EMBO J.* **10**, 3959-3970.

Nelson, G. A., Lew, K. and Ward, S. (1978). Intersex, a temperature sensitive mutant of the nematode *Caenorhabditis elegans*. *Dev. Biol.* **66**, 386-409.

Nelson, G. A. and Ward, S. (1980). Vesicle fusion, psuedopod extension, and amoeboid motility are induced in nematode spermatids by the ionophore monensin. *Cell* **19**, 457-464.

Nelson, G. A., Roberts, T. M. and Ward, S. (1982). *Caenorhabditis elegans* spermatozoan locomotion: amoeboid movement with almost no actin. *J. Cell Biol.* **92**, 121-131.

Okamoto, H. and Thomson, J. N. (1985). Monoclonal antibodies which distinguish certain classes of neuronal and supporting cells in the nervous tissue of the nematode *Caenorhabditis elegans*. *J. Neurosci.* **5**, 643-653.

Roberts, T. M., Pavalko, F. M. and Ward, S. (1986). Membrane and cytoplasmic proteins are transported in the same organelle complex during nematode spermatogenesis. *J. Cell Biol.* **102**, 1787-1796.

Rogaev, E. I., Sherrington, R., Rogaeva, E. A., Levesque, G., Ikeda, M., Liang, Y., Chi, H., Lin, C., Holman, K., Tsuda, T., et al. (1995). Familial Alzheimer's disease in kindreds with mis-sense mutations in a gene on chromosome 1 related to the Alzheimer's disease type 3 gene. *Nature* **376**, 775-778.

Rose, A. M. and Baille, D. L. (1980). Genetic organization of the region around *unc-15(I)*, a gene affecting paramyosin in *Caenorhabditis elegans*. *Genetics* **96**, 638-648.

Sale, W. S., Besharse, J. and Piperno, G. (1988). Distribution of acetylated α-tubulin in retina and *in vitro* assembled microtubules. *Cell Motil. Cytoskel.* **9**, 243-253.

Scheuner, D., Eckman, C., Jensen, M., Song, X., Citron, M., Suzuki, N., Bird, T. D., Hardy, J., Hutton, M., Kukull, W., et al. (1996). Secreted amyloid β-protein similar to that in the senile plaques of Alzheimer's disease is increases *in vivo* by the presenilin 1 and 2 and *APP* mutations linked to familial Alzheimer's disease. *Nature Med.* **2**, 864-870.

Shakes, D. C. (1988). Genetic and pharmacological analysis of spermatogenesis in the nematode *Caenorhabditis elegans*. PhD thesis, Johns Hopkins University, 189 pp.

Shakes, D. C. and Ward, S. (1989). Mutations that disrupt the morphogenesis and localization of a sperm-specific organelle in *Caenorhabditis elegans*. *Dev. Biol.* **134**, 307-316.

Shen, J., Bronson, R. T., Chen, D. F., Xia, W., Selkoe, D. J. and Tonegawa, S. (1997). Skeletal and CNS defects in *presenilin-1*-deficient mice. *Cell* **89**, 629-639.

Sherrington, R., Rogaev E., Liang, Y., Rogaeva, E. A., Levesque, G., Ikeda, M., Chi, H., Lin, C., Li, G., Holman, K., et al. (1995). Cloning of a gene bearing mis-sense mutations in early-onset familial Alzheimer's disease. *Nature* **375**, 754-760.

Sigurdson, D. C., Spanier, G. J. and Herman, R. K. (1984). *Caenorhabditis elegans* deficiency mapping. *Genetics* **108**, 331-345.

Smith, D. B. and Johnson, K. S. (1988). Single step purification of polypeptides expressed in *Escherichia coli* as fusions with glutathione S-transferase. *Gene* **67**, 31-40.

Stephens, R. E. (1986). Membrane tubulin. *Biol. Cell.* **57**, 95-110.

Taniguchi, T., Hashimoto, T., Taniguchi, R., Shimada, K., Kawamata, T., Yasuda, M., Nakai, M., Terashima, A., Koizumi, T., Maeda, K. and Tanaka, C. (1997). Cloning of the cDNA encoding rat presenilin-1. *Gene* **186**, 73-75.

Tomita, T., Maruyama, K., Saido, T. C., Kume, H., Shinozaki, K., Tokuhiro, S., Capell, A., Walter, J., Grunberg, J., Haass, C., Iwatsubo, T. and Obata, K. (1997). The presenilin 2 mutation (N1411) linked to familial Alzheimer's disease (Volga German families) increases the secretion of amyloid β protein ending at the 42nd (or 43rd) residue. *Proc. Nat. Acad. Sci. USA* **94**, 2025-2030.

Tsujimura, A., Yasojima, K. and Hashimoto-Gotoh, T. (1997). Cloning of *Xenopus* presenilin-α and -β cDNAs and their differential expression in oogenesis and embryogenesis. *Biochem. Biophys. Res. Commun.* **231**, 392-396.

Varkey, J. P., Muhlrad, P. J., Minniti, A. N., Do, B. and Ward, S. (1995). The *Caenorhabditis elegans spe-26* gene is necessary to form spermatids and encodes a protein similar to the actin-associated proteins kelch and scruin. *Genes Dev.* **9**, 1074-1086.

Ward, S. (1986). Asymmetric localization of gene products during the development of *Caenorhabditis elegans* spermatozoa. In *Gametogenesis and the Early Embryo* (ed. J. G. Gall), pp. 55-75. A. R. Liss, Inc., New York.

Ward, S., Argon, Y. and Nelson, G. A. (1981). Sperm morphogenesis in wild-type and fertilization-defective mutants of *Caenorhabditis elegans*. *J. Cell Biol.* **91**, 26-44.

Ward, S., Roberts, T. M., Strome, S., Pavalko, F. and Hogan, E. (1986). Monoclonal antibodies that recognize a polypeptide antigenic determinant shared by multiple *Caenorhabditis elegans* sperm-specific proteins. *J. Cell Biol.* **102**, 1778-1786.

Waterston, R. H. (1980). A second informational suppressor *sup-7 X*, in *Caenorhabditis elegans*. *Genetics* **97**, 307-325.

Wolf, N., Hirsh, D. and McIntosh, J. R. (1978). Spermatogenesis in males of the free-living nematode, *Caenorhabditis elegans*. *J. Ultrastruct. Res.* **63**, 155-169.

Wong, P. C., Zheng, H., Chen, H., Becher, M. W., Sirinathsinghji, D. J. S., Trumbauer, M. E., Chen, H. Y., Price, D. L., Van der Ploeg, L. H. T. and Sisodia, S. (1997). Presenilin 1 is required for *Notch1* and *Dll1* expression in the paraxial mesoderm. *Nature* **387**, 288-292.